

## Monitoring drought effects on vegetation water content and fluxes in chaparral with the 970 nm water band index

Helen C. Claudio\*, Yufu Cheng, David A. Fuentes, John A. Gamon, Hongyan Luo, Walter Oechel, Hong-Lie Qiu, Abdullah F. Rahman, Daniel A. Sims

*California State University, Los Angeles Los Angeles, CA, USA*

Received 10 May 2004; received in revised form 22 July 2005; accepted 24 July 2005

### Abstract

The goal of this study was to explore the utility of the 970 nm water band index (WBI) in estimating evapotranspiration and vegetation water status for a semiarid shrubland ecosystem. Between 2001 and 2003, spectral reflectance coupled with CO<sub>2</sub> and water flux data were collected at Sky Oaks Biological Field Station, a chaparral-dominated ecosystem in southern California, and one of the sites within the SpecNet network. The reflectance data were collected either by walking along a 100 m transect or by using a semi-automated tram system installed later at the site along the same 100 m transect. CO<sub>2</sub> and water flux data were gathered with an eddy covariance flux tower adjacent to the tram system. The 970 nm WBI and normalized difference vegetation index (NDVI) were derived from the spectral reflectance. The two indices were expressed both as points approximately a meter apart along the transect and as whole-transect averages, where all of the reflectance values along the transect were averaged together, simulating a large pixel. This study encompassed a wet year with normal precipitation (2001), a 100-year record drought (2002), and a recovery year (2003), allowing for comparison over time and between precipitation regimes. Species-specific responses to wet and dry periods were evident in the reflectance spectra, providing a basis for separating species based on their optical properties. The WBI was significantly correlated with the NDVI revealing a strong link between canopy water content and green canopy structure; however this relationship varied with species and water status, providing evidence for the independence of these two optical indices. The WBI was also strongly linked to surface–atmosphere fluxes, explaining 49% of the variance in the water vapor flux, and 24% of the carbon dioxide fluxes. These results suggest that WBI or other similar water status indices may be useful variables in modeling CO<sub>2</sub> and water fluxes when combined with other physiological, environmental, and atmospheric factors.

© 2006 Published by Elsevier Inc.

*Keywords:* Chaparral; Water band index; Meter resolution measurement; Evapotranspiration; Drought temporal dynamics

### 1. Introduction

Evapotranspiration, the combination of evaporation and transpiration, is an important component of the water cycle. Evapotranspiration rates vary with water availability and physiological status, providing a potent indicator of vegetation stress and productivity. Furthermore, evapotranspiration plays a role in regional and global climate by influencing heat exchange and cloud formation. Understanding the patterns and controls involved will allow for more efficient water use, particularly with respect to general land use, crop irrigation, and planning

for droughts. This is especially critical in arid regions and other areas that are drought-prone, where water is especially limited due to lack of precipitation and possibly high temperatures or low relative humidity.

While evapotranspiration can be directly measured by methods such as eddy covariance, this measurement is generally limited to relatively small, flat regions. It is also impractical to install a network of eddy towers to cover large areas of land. Thus, for large regions, there is a need to apply remote sensing to detect patterns in evapotranspiration. This study explores the ability of spectral reflectance to detect spatial and temporal patterns of evapotranspiration

Reflectance spectra present many possible water indices because there are several water absorption features in the near- and far-infrared region (Sims & Gamon, 2003; Serrano et al.,

\* Corresponding author.

*E-mail addresses:* [greywolf@alumni.caltech.edu](mailto:greywolf@alumni.caltech.edu), [hclaudi@calstatela.edu](mailto:hclaudi@calstatela.edu) (H.C. Claudio).

2000). Among these water indices are the water band index (WBI, also called the water index; Peñuelas et al., 1993), the shortwave infrared water stress index (SIWSI, derived from MODIS near- and shortwave infrared bands; Fensholt & Sandholt, 2003), three-band ratio indices (RATIO<sub>975</sub> and RATIO<sub>1200</sub>; Pu et al., 2003), equivalent water thickness (EWT; Roberts et al., 1998; Serrano et al., 2000; Sims & Gamon, 2003), and the normalized difference water index (NDWI; Gao, 1996; Serrano et al., 2000).

A number of studies have searched for optimal formulas and wavelengths, often from a theoretical perspective, but there has been relatively little validation with field data (Fensholt & Sandholt, 2003; Pu et al., 2003; Serrano et al., 2000; Sims & Gamon, 2003). Consequently, the search for an optimal water band or expression of reflectance to yield a measure of vegetation water status has been elusive. The longer wavelengths, such as the 1450 and 1900 nm water absorption bands, make poor indicators for estimating plant water content due to the low incoming solar energy and high levels of interference by atmospheric water vapor (Sims & Gamon, 2003). There is insufficient energy available for these longer wavelengths to be practical for vegetation water content. Several studies suggest that the ideal wavelengths for predicting water content are wavelengths with weak absorption coefficients that allow the radiation to penetrate far into canopies, providing a suitable dynamic range (Peñuelas et al., 1993; Roberts et al., 1997; Sims & Gamon, 2003). For example, recent studies have suggested that the weakly absorbing 970 nm and 1200 nm regions, provide suitable wavebands for monitoring plant canopy water content (Serrano et al., 2000; Sims & Gamon, 2003).

Often, the choice of water band is further limited by practical issues, including the detector and foreoptics used, and the atmospheric conditions at the time of sampling. For example, many silicon photodiode sensors have upper detection limits around 1100 nm, so they can only obtain the first band (970 nm region). Strong absorption due to atmospheric water vapor may often render some water bands useless for aircraft and satellite remote sensing, particularly at longer wavelengths, where water vapor absorbs most strongly. Because of small differences in the wavelength of maximum absorption in the water vapor and liquid water bands, hyperspectral instruments (e.g. AVIRIS) can distinguish water vapor from liquid water for a number of the water bands, and a good atmospheric correction can reveal a true surface reflectance, but only under fairly optimal, clear sky conditions (Green et al., 1998). “Full range” field instruments exist that can sample out to 2500 nm, but these are quite expensive, bulky, more subject to calibration errors than silicon photodiode sensors, and not readily adaptable to automated, mobile sampling. Thus, from a practical perspective, we are often limited in field sampling to the 970 nm water band. This, combined with the wide availability, low cost, and portability of silicon photodiode sensors, is why we explored the 970 nm WBI as an indicator of water fluxes.

The WBI is calculated as  $R_{900}/R_{970}$ , where  $R_x$  is the reflectance at a given wavelength and the bandwidth (FWHM) is typically 10 nm. This index utilizing the ratio of  $R_{900}$  and  $R_{970}$  was first introduced as a plant water index (WI)

by Peñuelas et al. (1993). Past studies have indicated that it provides a good indicator of water content in the fine tissues of the canopy (Sims & Gamon, 2003), particularly in green leaves (Peñuelas et al., 1993), and can also be an indicator of the leaf area index (LAI; Gamon & Qiu, 1999; Roberts et al., 1998). Other studies (Mo et al., 2004; Zarco-Tejada et al., 2003) have also indicated that it is possible to model water balance and content through reflectance data. Zarco-Tejada et al. assessed the use of plant water index (PWI) derived from MODIS data in modeling vegetation water content and found that the MODIS estimates were strongly correlated with ground and field measurements of water content. Mo et al. used NDVI data to model evapotranspiration, with simulated fluxes closely matching measured fluxes. In addition to estimating water content, WBI can be used to track changes associated with vegetation cover and season in both field and AVIRIS data sets (Gamon & Qiu, 1999; Gamon et al., 1998; Serrano et al., 2000). However, to our knowledge, there have been few studies investigating the relationship between a water band signal and evapotranspiration.

Since chaparral phenology and productivity are closely tied to water status (Baker et al., 1982), remote measures of water status would be useful in monitoring seasonal and drought effects. The purpose of this study was to explore the utility of the WBI as a direct indicator of water status and evapotranspiration in this ecosystem.

## 2. Methods

Sky Oaks is a chaparral site located in northern San Diego County (33°22'N, 116°37.2'W) and is part of a developing network known as SpecNet (Spectral Network). A primary goal of SpecNet is to integrate optical and flux data to gain insights into the factors controlling carbon dioxide and water vapor fluxes across contrasting ecosystems. The study site had gone unburned for nearly a century. In 2002, the site underwent a 100-year record drought, bracketed by 2 years of near-normal precipitation, creating an opportunity to observe ecosystem changes through extreme precipitation conditions. At this site, the dominant species were chamise (*Adenostoma fasciculatum*), redshank (*Adenostoma sparsifolium*), and manzanita (*Arctostaphylos pungens*).

Reflectance data were collected starting in 2000 and are currently ongoing, although this report focused on data from a 2.5-year period spanning January 2001 to July 2003, prior to a wildfire that destroyed all sampling equipment and above-ground vegetation. The data were taken by a dual detector spectrometer (UnispecDC, PP Systems, Amesbury, MA, USA) capable of correcting for changing sky conditions by taking readings both of the sky and of the target and normalizing based on sky conditions (Gamon et al., 2006-this issue). This was accomplished by having one detector foreoptic looking upwards to sample sky irradiance, and the other detector foreoptic looking downwards to sample reflected radiance. At the beginning of every transect run, these two detectors were cross calibrated using a 99% reflective target (Spectralon, Labsphere Inc., North Sutton, NH, USA).

In the early phase of this study, optical data were taken manually, by walking with the spectrometer along a 55- or 100-m transect (Table 1) and taking measurements at every meter. During manual data collection, the downward-looking foreoptic was positioned approximately 3 m above the ground, yielding an instantaneous field of view (IFOV) of approximately one meter diameter on the ground. Starting in May, 2001, reflectance data were collected along the identical 100-m transect by mounting the spectrometer on a “tram system”, consisting of a robotic cart traveling on a 100-m track, and allowing unattended, automatic operation (and thus avoiding disturbance of the vegetation). When using the tram, the downward-looking foreoptic was positioned at 3–4.5 m above the canopy surface (distance varying slightly with topography), yielding an IFOV of approximately 1–1.5 m.

The transect was located near the footprint of an eddy flux tower and the tram was run periodically, typically 1 or 2 days a month. By taking data points at set spatial intervals (i.e., every meter), it was possible to sample individual plant species or cover types. It was also possible to have several replicates of the same species fall along a single sampling pass, allowing analysis of species-specific responses. Alternatively, reflectance for the entire landscape could be averaged, creating a synthetic “large pixel” index value for the entire ecosystem that could then be compared to flux data, or remotely sensed data (Cheng et al., 2006-this issue). On each sampling date, measurements were taken several times a day during daylight hours and recorded on a laptop aboard the cart, but all data used in this study were the averaged midday readings (10:00 h–14:00 PST).

Reflectance data were processed with a software package that corrected and interpolated the readings to one nm intervals (Multispec, available on [http://vcsars.calstatela.edu/lab\\_documents/mspec.html](http://vcsars.calstatela.edu/lab_documents/mspec.html)) and then archived into spreadsheets. Using the reflectance data, WBI was calculated as

$$R_{900}/R_{970}$$

(Peñuelas et al., 1997), and NDVI was calculated as

$$(R_{800} - R_{680}) / (R_{800} + R_{680})$$

where  $R$  indicates reflectance, and the subscript indicates a particular wavelength in nm.

Table 1

Summary of whether transect reflectance was sampled manually or automatically via the tram system, the distance sampled (55 or 100 m), the type of infrared gas analyzer (IRGA) on the eddy covariance system, and how the data were used (for the time series only or for all analyses, including correlation)

Dates	Reflectance method	Distance measured (m)	IRGA	Analyses
1/18/2001–4/18/2001	Manual	55	LI-6262	Time series
5/7/2001	Manual	100	LI-6262	Time series
5/25/2001–10/25/2001	Tram	100	LI-6262	Time series
10/25/2001–7/10/2003	Tram	100	LI-7500	All

The LI-6262 was a closed-path IRGA on the eddy covariance system, which was replaced by the LI-7500, an open-path IRGA.

The statistical analyses performed were simple correlations using appropriate statistical packages such as SPSS or StatView. Throughout the paper, the value of  $\alpha$  is at the 0.05 level for determining whether a correlation was significant. Also, least squares regressions were used to determine the effects of species and season on the correlations between NDVI and WBI. These regressions were then analyzed using ANCOVA to determine whether the slopes were significantly different and then post-hoc Tukey’s test was done to determine which slopes were different if there were any significant differences.

Carbon dioxide (CO<sub>2</sub>) and water flux data were gathered using an eddy covariance tower with an IRGA CO<sub>2</sub> detection device and meteorological instruments (see Sims et al., 2006-this issue, for details of the eddy covariance methods). Prior to October of 2001, the flux measurements were made using a closed-path IRGA (LI-6262, LI-COR, Lincoln, NE, USA). Starting in October, 2001, this was replaced by a more stable, open-path IRGA (LI-7500). While all flux data were used to show the time series, only flux data from the more stable, open-path IRGA readings were used for correlation analyses (Table 1). The eddy tower was maintained by the Global Change Research Group at San Diego State University as part of the Ameriflux network, and the daily 24-h averaged flux data were downloaded from the GCRG website (<http://www.sci.sdsu.edu/GCRG/>, “Online Data Pages”). These data were obtained directly from the website “as is” and received no further processing.

Simultaneous sampling of CO<sub>2</sub> and H<sub>2</sub>O fluxes and reflectance from 2001 to 2003 allowed for comparisons exploring the dynamics of water status in the ecosystem. Correlation analyses were performed on fluxes and indices, and the effects of precipitation and species were also investigated. The correlation analyses included NDVI–WBI correlations (by species, time, and transect averages) and CO<sub>2</sub> flux and H<sub>2</sub>O flux vs. WBI correlations. NDVI and WBI data were also simultaneously compared along the transect and through time with emphasis on species type (*Adenostoma* species and *Arctostaphylos*).

### 3. Results

Each species had its own spectral reflectance pattern, both in drought and non-drought periods, as shown in Fig. 1. During the wet year, the vegetation spectra exhibited a steep slope at the “red edge” region and a conspicuous depression between 900 and 1000 nm, leading to large NDVI and WBI values, respectively. During the drought period, the steep slope at 700 nm relaxed, as did the 970 nm depression, indicating low NDVI and WBI. *Arctostaphylos* in particular took on a more linear shape during the drought, while the *Adenostoma* species retained the red-edge inflection near 700 nm characteristic of green canopies. The spectrum of the soil background also exhibited large seasonal changes in brightness, which were attributable to seasonal changes in sun angle, with the soil appearing brighter in June when the sun was higher above the horizon.

Along the transect, distinct NDVI and WBI peaks corresponded to individual shrub locations (Fig. 2). Prior to the

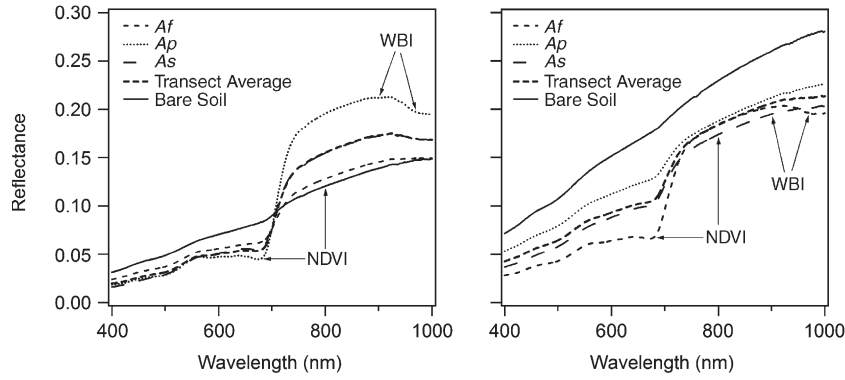


Fig. 1. Typical reflectance spectra for each species (*Af*=*Adenostoma fasciculatum*, *Ap*=*Arctostaphylos pungens*, *As*=*Adenostoma sparsifolium*). To the left are the pre-drought reflectance spectra and to the right are the drought spectra, taken December 2001 and June 2002, respectively. The wavelengths used for the two reflectance indices, NDVI (normalized difference reflectance index) and WBI (water band index), are also shown. The different species and the bare soil are averages of that particular cover type from a single transect run at mid-day and all available points for each given cover type (10 for soil, 40 for *Af*, 15 for *Ap*, and 10 for *As*).

drought, *Arctostaphylos*, shown as discrete peaks, had the highest NDVI and WBI readings, while *A. fasciculatum* and *A. sparsifolium* showed lower readings. During the drought, most of the vegetation WBI and NDVI values declined, indicating less water and green leaf area, respectively. By comparing the December (pre-drought) and June (drought) NDVI and WBI, it is possible to explore moisture effects on individual shrubs. Note, however, that sun angle effects (considered in detail in Sims et al., 2006-this issue) can also influence index values. In particular, part of the seasonal NDVI shifts shown in Fig. 2 can be attributed to the changes in solar angle. Thus, to fully clarify the drought effect on the index values of individual targets along the transect, corrections for sun angle must also be considered (Sims et al., 2006-this issue).

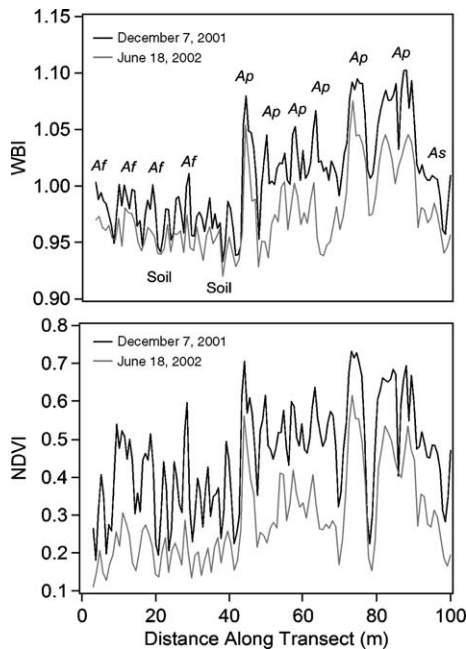


Fig. 2. Transect NDVI and WBI under wet and drought conditions. Note that different species have different peaks at different times due to varying greenness (NDVI) and water status (WBI). Individual shrubs appear as distinct, individual peaks, especially in the case of *Arctostaphylos* (*Af*=*Adenostoma fasciculatum*, *Ap*=*Arctostaphylos pungens*, *As*=*Adenostoma sparsifolium*).

In general, optical indices (WBI and NDVI) closely matched the temporal dynamics of precipitation and water vapor fluxes. In 2001–2002, there were coincident winter wet season peaks in NDVI, WBI, and water flux, and troughs in all of these features in the summer dry seasons (Fig. 3). The small amount of precipitation in winter 2002 indicated a drought year (the driest on record for this site, according to unpublished data from local weather stations), and WBI and water vapor fluxes were both reduced in 2002 relative to the previous winter (2001). During the summer of 2002, a large amount of dieback occurred in this normally evergreen chaparral stand, and this was visible in the decline in NDVI (green leaf area) through the summer of 2002. During the summer drought of 2002, precipitation, NDVI, WBI, and water flux all reached minima. In winter 2003, following this severe drought, there was a slight recovery of WBI and water vapor flux following a return of normal precipitation levels, and this response was coincident with a slight increase in NDVI indicating canopy regrowth. Field observations

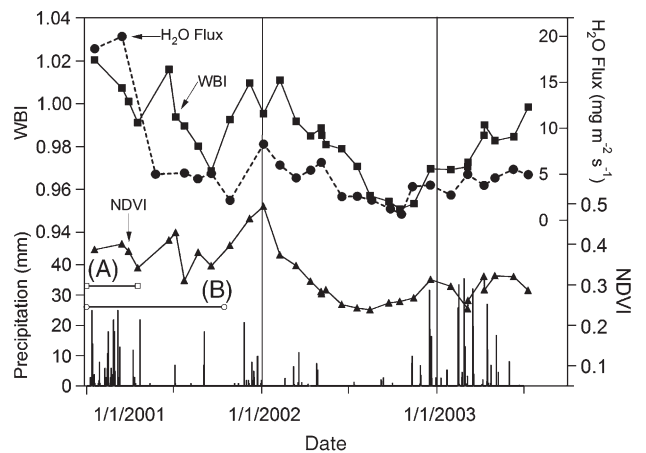


Fig. 3. Precipitation, water flux, and water band index (WBI) over time from January 2001 to July 2003. Note the seasonal variations in WBI, NDVI, and the water flux. Also note the low NDVI and WBI during the drought period (summer 2002) compared to previous and following years: (A) the time period of manual reflectance sampling; (B) the time period of the closed-path IRGA (not used for correlation analysis, Table 1).

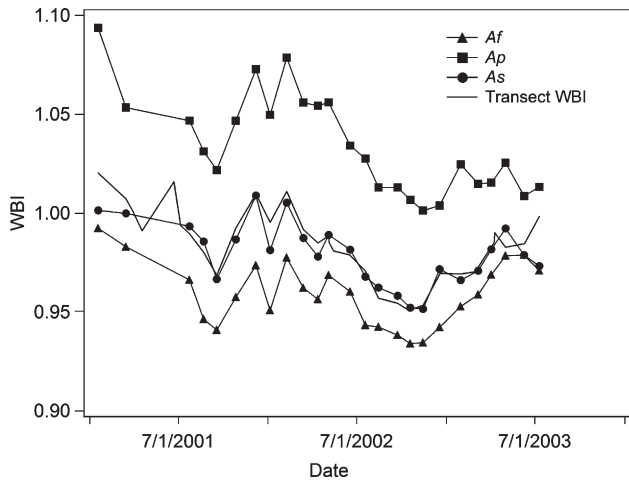


Fig. 4. The WBI measurements of the overall transect average (all species combined) and the three individual dominant species (*Adenostoma fasciculatum*, *Adenostoma sparsifolium*, and *Arctostaphylos pungens*) at Sky Oaks over time from January 2001 to July 2003.

indicated that this recovery was limited by substantial shrub dieback, which varied between species, as further discussed below.

The magnitude of the water band index response varied across the three dominant species at Sky Oaks (Fig. 4). Although all three of the species followed similar dynamics, the magnitudes in WBI values varied between species, and the rate of recovery following drought also differed due to species-specific drought responses. For *A. fasciculatum* and *A. sparsifolium*, the WBI readings were of relatively low magnitude, and both appear to have been recovering in 2003, following heavy winter rains. For *Arctostaphylos*, the magnitudes of the WBI were larger during the wet year (2001) and the WBI level did not increase very much during the post-drought recovery period (2003) as it did with the other two species. Field

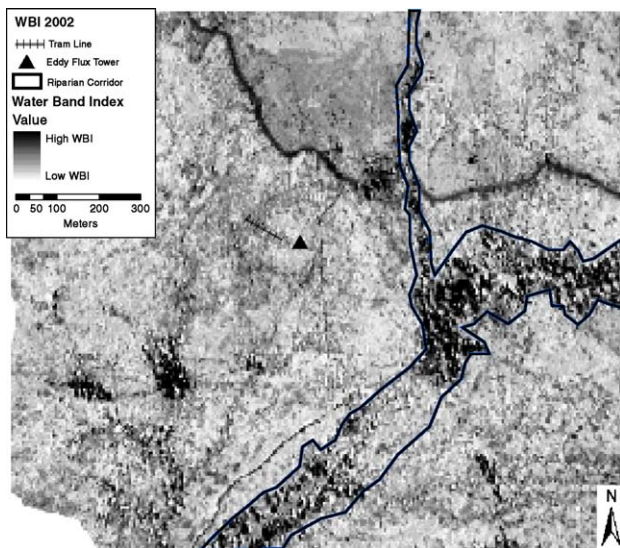


Fig. 5. Transformed AVIRIS image to show WBI. Image was taken on October 3, 2002. Darker areas indicate areas of high relative WBI, while lighter areas indicate low WBI.

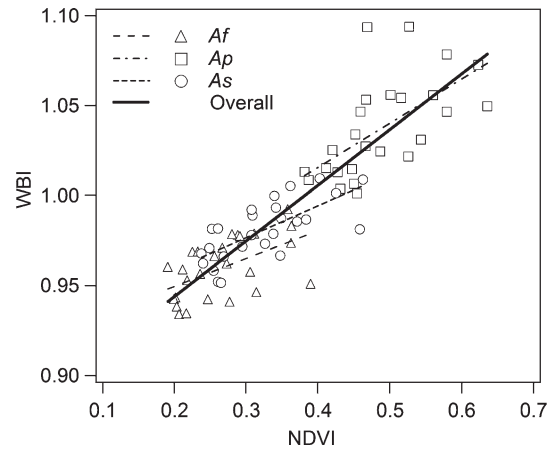


Fig. 6. NDVI vs. WBI for *Adenostoma fasciculatum* (*Af*), *Arctostaphylos pungens* (*Ap*), and *Adenostoma sparsifolium*, as well as the overall correlation for all species together, from reflectance data collected between March 2001 and July 2003.  $r^2=0.782$ ,  $p<0.0001$ , slope=0.301 overall,  $r^2=0.295$ ,  $p=0.0042$ , slope=0.155 for *Adenostoma fasciculatum*,  $r^2=0.389$ ,  $p=0.0007$ , slope=0.246 for *Arctostaphylos pungens*,  $r^2=0.502$ ,  $p<0.0001$ , slope=0.177 for *Adenostoma sparsifolium*. There was a significant difference among the slopes (ANCOVA:  $F=47.6186$ ,  $p<0.0001$ ) with significant differences between *Af* and *Ap* ( $q=13.690$ ) and *As* and *Ap* ( $q=9.921$ ) at the 0.05 significance level (Tukey's test:  $q_{crit}=3.399$ ).

investigations conducted during the drought revealed that several of the *Arctostaphylos* shrubs had died completely, while the *A. fasciculatum* and *A. sparsifolium* experienced only partial dieback (individual dead branches scattered within living canopies), which accounted for the interspecific differences during the recovery phase.

Spatial patterns of WBI revealed contrasts in areas with different species cover (Fig. 5). Along the tram line, subtle

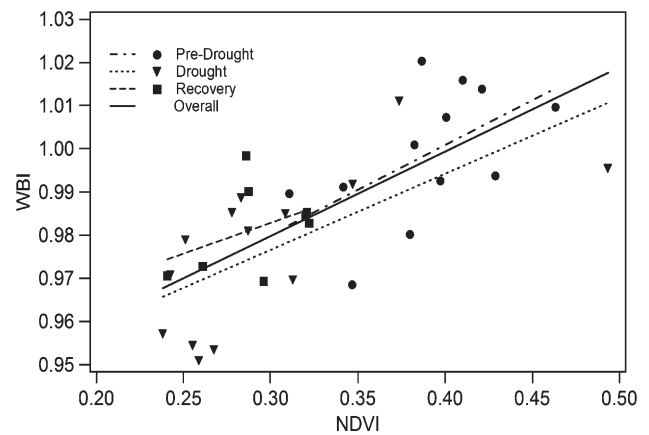


Fig. 7. NDVI vs. WBI for transect average data, from reflectance data collected between January 2001 and July 2003, with different symbols indicating different time periods. The predrought period was before January 2002, while the drought was from January 2002 until July 2003. Correlations and significances of the individual time frames are respectively: pre-drought ( $r^2=0.311$ ,  $p=0.0595$ , slope=0.208), drought ( $r^2=0.443$ ,  $p=0.0094$ , slope=0.176), recovery ( $r^2=0.443$ ,  $p=0.0094$ , slope=-0.176). The overall correlation and correlation for all dates together was highly significant ( $r^2=0.533$ ,  $p<0.0001$ , slope=0.195). There was a significance difference among the slopes (ANCOVA:  $F=6.486$ ,  $p<0.0001$ ). The pre-drought and drought ( $q=4.11$ ) and the predrought and drought recovery ( $q=7.67$ ) were significantly different from each other ( $q_{crit}=3.339$ ).

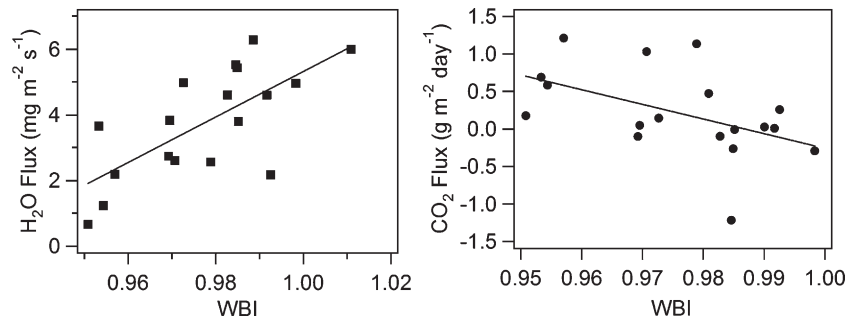


Fig. 8. Correlations between  $\text{CO}_2$  and  $\text{H}_2\text{O}$  fluxes with transect average WBI respectively. Note the stronger correlation between WBI and  $\text{H}_2\text{O}$  flux than with  $\text{CO}_2$  flux. For the  $\text{CO}_2$  flux, negative values indicate uptake into the ecosystem, while positive values indicate loss into atmosphere.  $\text{H}_2\text{O}$ –WBI:  $r^2=0.492$ ,  $p=0.0012$ .  $\text{CO}_2$ –WBI:  $r^2=0.238$ ,  $p=0.040$ .

differences are apparent between the tower end (meter 0) and the western end (meter 100), with slightly higher values apparent towards the west end of the tram, associated with the transition from *A. fasciculatum* to *A. pungens* and *A. sparsifolium* (see Fig. 2). The riparian corridor, which was dominated by *Quercus agrifolia*, clearly shows up as a darker (higher WBI) region.

Strong correlations existed between NDVI and WBI (Figs. 6 and 7), and different species occupied different regions within WBI–NDVI space as shown in Fig. 6, reflecting interspecific differences in canopy structure and water status. For example, *A. fasciculatum* was in the region of lower NDVI and WBI, while the *Arctostaphylos* occupied the higher NDVI and WBI regions. The slope for *A. pungens*, the species that died in drought, was significantly different from that of each of the other species (Fig. 6).

The correlations between NDVI and WBI across time were also significant (see Fig. 7 caption for statistical values), although the correlation was greater when all species were combined than when each individual species was examined separately (not shown). The post-drought data points typically were in the region of low NDVI and WBI, while the pre-drought data points were typically in the higher NDVI and WBI regions. Significant differences in WBI–NDVI slopes were apparent, with the pre-drought slope significantly different from that of the drought and recovery phases (Fig. 7). Additionally, during drought, there was a downward shift in this relationship (lower WBI values for a given NDVI), presumably reflecting the changing moisture status of the vegetation.

There was considerable scatter in the WBI–flux relationships. However, WBI was significantly correlated with both water vapor and  $\text{CO}_2$  fluxes, and the correlation with water flux was stronger (Fig. 8).

#### 4. Discussion and conclusions

The ability of WBI and NDVI on each point of the transect to distinguish different species in the ecosystem is consistent with past studies (Gamon & Qiu, 1999; Serrano et al., 2000), indicating NDVI and WBI responses vary with vegetation type and physiological status, allowing these indices to be used for functional vegetation mapping (Fuentes

et al., 2001). The 1-m resolution (IFOV – pixel size or grain size) of reflectance measurements made along the transect allowed us to explore individual species responses. With the ability to go from the fine (individual shrub, 1-m IFOV) to the coarse (whole stand, 100-m span) it is possible to identify individual species contributions to the whole-stand flux and optical responses.

The repeated tram sampling allowed us to monitor individual shrub decline and recovery. Differential species sensitivity to drought was clearly apparent in the larger decline in *Arctostaphylos* WBI, NDVI and cover during drought (all individuals of this species died). With most remotely sensed data (e.g. MODIS), the pixel resolution is much larger making it impossible to identify individual shrubs or even very small stands. Thus, the tram provides a useful tool for evaluating changes in species composition, and the varying contribution of individual species to the overall reflectance of a vegetation stand.

The marked change in NDVI, WBI, and spectral reflectance with drought and recovery indicate that vegetation water status strongly influences optical properties detectable with hyperspectral remote sensing. It also shows that chaparral ecosystem metabolism and water vapor fluxes, like other drought-prone ecosystems (e.g. Fensholt & Sandholt, 2003), are strongly driven by the presence or absence of water. Based on past studies (Gamon et al., 1995), it would be expected that the NDVI would decrease as water became less available because NDVI is an indicator of green leaf area (Sims & Gamon, 2003), which can vary with vegetation water content (Peñuelas et al., 1997). Similarly, WBI, which provides an indicator of water content in leaves and other thin tissues (Sims & Gamon, 2003), varies in concert with NDVI. Others have suggested that, like NDVI, water indices may provide a measure of leaf area index (Roberts et al., 1998). Note, however, that the NDVI and WBI are not identical, as illustrated by the different NDVI–WBI regressions for different species or for different phases of water availability. Presumably, these unique NDVI–WBI responses provide useful indicators of structural and physiological differences, providing a subtle, but potentially powerful, way to distinguish functionally distinct vegetation types and drought responses.

With decreasing water availability during drought, plant water content, reducing the WBI and similar water content

signals, as shown in other studies (Serrano et al., 2000; Sims & Gamon, 2003; Peñuelas et al., 1997; Pu et al., 2003). In parallel, evapotranspiration also decreased, presumably because water-stressed plants shut their stomata and dropped leaves to conserve water. In severe drought (2002), field observations indicated that extensive shrub dieback accounted for much of the reduction in WBI and evapotranspiration, and this reduction was species-dependent.

The greater decline of *A. pungens* during drought may be partly due to its different leaf structure. *A. fasciculatum* and *A. sparsifolium* have relatively small, needle-shaped leaves, which are suited for water conservation since they are better coupled to the atmosphere and thus tend to have lower temperatures under high radiation loads, which results in lower transpiration. *Arctostaphylos* leaves have greater surface area, resulting in higher leaf temperatures, which may have become lethal during the extreme drought. *A. fasciculatum* and *A. sparsifolium* are also semi-deciduous, meaning that they can lose part of their leaves during a drought, thus reducing their transpiration, whereas *Arctostaphylos* appears to lack the ability for selective leaf abscission. Also, root structure and water use will affect the chances of survival in a drought. *Arctostaphylos* generally has a shallower root system than the *Adenostoma* species (Hart & Radosevich, 1987). With a deeper root system, it is possible for the shrub to extract water from deeper soil layers during drought periods.

Clearly, the water band index (WBI) is dynamic over time and space and varies with different plant species and precipitation regimes. The strong correlation between the WBI and the water and carbon fluxes indicates that the WBI can be used to estimate both fluxes, especially the water flux. With the proper hyperspectral imagery, it is then possible to create empirically calibrated “flux maps” of the region (Fuentes et al., 2006-this issue). To produce a mechanistic, or process, model, the leaf-to-air vapor pressure deficit, stomatal resistance, and boundary layer resistance would be needed. Since VPD varies with surface and air temperature, it is possible that surface temperature (also remotely detectable) would be useful. A few models, particularly SiB2, already utilize physiological parameters such as stomatal resistance (Collatz et al., 1992; Sellers et al., 1996a,b), but the additional parameters required by these models often restrict their usage to regions where extensive physiological data are already available. We are currently working on a mechanistic model incorporating some of these additional factors to see if it can improve the ability to predict evapotranspiration with WBI as an input. The value of this approach is that it can be driven by remotely sensed inputs and thus used to assess both temporal and spatially changing water vapor fluxes.

## Acknowledgements

This research was funded by three grants from the National Science Foundation (CEA-CREST, NSF-Ecosystem and NSF-SGER) awarded to Dr. John Gamon. Thanks go to CEA-CREST and NSF-Ecosystem funded students who helped in the data collection and tram construction.

## References

- Baker, G. A., Rundel, P. W., & Parsons, D. J. (1982). Comparative phenology and growth in three chaparral shrubs. *Botanical Gazette*, *143* (1), 94–100.
- Cheng, Y., Gamon, J. A., Fuentes, D. A., Mao, Z., Sims, D. A., Qiu, H. -L., et al. (2006). A multi-scale analysis of dynamic optical signals in a Southern California chaparral ecosystem: a comparison of field, AVIRIS and MODIS data. *Remote Sensing of Environment*, *103*, 369–378 (this issue). doi:10.1016/j.rse.2005.06.013
- Collatz, G. J., Ribas-Carbo, M., & Berry, J. A. (1992). Coupled photosynthesis–stomatal conductance model for leaves of C4 plants. *Australian Journal of Plant Physiology*, *19*, 519–513.
- Fensholt, R., & Sandholt, I. (2003). Derivation of a shortwave infrared water stress index from MODIS near- and shortwave infrared data in a semiarid environment. *Remote Sensing of Environment*, *87*, 111–121.
- Fuentes, D. A., Gamon, J. A., Cheng, Y., Qiu, H. -L., Mao, Z., Sims, D. A., et al. (2006). Mapping carbon and water flux in a chaparral ecosystem using vegetation indices derived from AVIRIS. *Remote Sensing of Environment*, *103*, 312–323 (this issue). doi:10.1016/j.rse.2005.10.028
- Fuentes, D. A., Gamon, J. A., Qiu, H. -L., Sims, D. A., & Roberts, D. A. (2001). Mapping Canadian boreal forest vegetation using pigment and water absorption features derived from the AVIRIS sensor. *Journal of Geophysical Research*, *106*(D24), 33,565–33,577.
- Gamon, J. A., et al. (2006). A mobile tram system for systematic sampling of ecosystem optical properties. *Remote Sensing of Environment*, *103*, 246–254 (this issue). doi:10.1016/j.rse.2006.04.006
- Gamon, J. A., Field, C. B., Goulden, M. L., Griffin, K. L., Hartley, A. E., Joel, G., et al. (1995). Relationships between NDVI, canopy structures, and photosynthesis in three Californian vegetation types. *Ecological Applications*, *5*, 28–41.
- Gamon, J. A., Lee, L. -F., Qiu, H. -L., Davis, S., Roberts, D. A., Ustin, S. L. (1998). A multi-scale sampling strategy for detecting physiologically significant signals in AVIRIS imagery. In *Summaries of the 7th Annual JPL Earth Science Workshop, 12–16 January*. Pasadena, CA, JPL publication 97-21, 1 111–120.
- Gamon, J. A., & Qiu, H. -L. (1999). Ecological applications of remote sensing at multiple scales. In F. I. Pugnaire, & F. I. Valladares (Eds.), *Handbook of functional plant ecology* (pp. 805–845). New York: Marcel Dekker.
- Gao, B. -C. (1996). NDWI – a normalized difference index for remote sensing of vegetation liquid water from space. *Remote Sensing of Environment*, *52*, 155–162.
- Green, R. O., Eastwood, M. L., Sarture, C. M., Chrien, T. G., Aronsson, M., Chippendale, B. J., et al. (1998). Imaging spectroscopy and the airborne visible/infrared imaging spectrometer. *Remote Sensing of Environment*, *65*, 227–248.
- Hart, J. H., & Radosevich, S. R. (1987). Water relations of two California chaparral shrubs. *American Journal of Botany*, *74*(3), 371–384.
- Mo, X., Liu, S., Lin, Z., & Zhao, W. (2004). Simulating temporal and spatial variation of evapotranspiration over the Lushi basin. *Journal of Hydrology*, *285*, 125–142.
- Peñuelas, J., Filella, I., Biel, C., Serrano, L., & Save, R. (1993). The reflectance at the 950–970 nm region as an indicator of plant water status. *International Journal of Remote Sensing*, *14*, 1887–1905.
- Peñuelas, J., Pinol, J., Ogaya, R., & Filella, I. (1997). Estimation of plant water concentration by the reflectance water index WI ( $R_{900}/R_{970}$ ). *International Journal of Remote Sensing*, *14*, 1887–1905.
- Pu, R., Ge, S., Kelly, N. M., & Gong, P. (2003). Spectral absorption features as indicators of water status in coast live oak (*Quercus agrifolia*) leaves. *International Journal of Remote Sensing*, *24*, 1799–1810.
- Roberts, D. A., Brown, K., Green, R. O., Ustin, S. L., & Hinckley, T. (1998). Investigating the relationships between liquid water and leaf area in clonal *Populus*. *Summaries of the 7th annual JPL Earth Science Workshop, January 12–16, 1998, Pasadena, CA, vol. 1* (pp. 335–344). JPL Publication 97-21 Available at: [http://popo.jpl.nasa.gov/docs/workshops/98\\_docs/toc.html](http://popo.jpl.nasa.gov/docs/workshops/98_docs/toc.html)
- Roberts, D. A., Green, R. O., & Adams, J. B. (1997). Temporal and spatial patterns in vegetation and atmospheric properties from AVIRIS. *Remote Sensing of Environment*, *62*, 223–240.

- Sellers, P. J., Collatz, G. J., & Randal, D. R. (1996). A revised land-surface parameterization (SiB<sub>2</sub>) for GCMs: Part 1. Model formulation. *Journal of Climate*, 9, 706–737.
- Sellers, P. J., Los, S. O., & Tucker, C. J. (1996). A revised land-surface parameterization (SiB<sub>2</sub>) for GCMs: Part 2. The generation of global fields of terrestrial biophysical parameters from satellite data. *Journal of Climate*, 9, 676–736.
- Serrano, L., Ustin, S. L., Roberts, D. A., Gamon, J. A., & Peñuelas, J. (2000). Deriving water content of chaparral vegetation from AVIRIS data. *Remote Sensing of Environment*, 74, 570–581.
- Sims, D. A., & Gamon, J. A. (2003). Estimation of vegetation water content and photosynthetic tissue area from spectral reflectance: a comparison of indices based on liquid water and chlorophyll absorption features. *Remote Sensing of Environment*, 84, 526–537.
- Sims, D. A., Luo, H., Hastings, S., Oechel, W. C., Rahman, A., & Gamon, J. A. (2006). Parallel adjustments in vegetation greenness and ecosystem CO<sub>2</sub> exchange in response to drought in a Southern California chaparral ecosystem. *Remote Sensing of Environment*, 103, 289–303 (this issue). doi:10.1016/j.rse.2005.01.020
- Zarco-Tejada, P. J., Rueda, C. A., & Ustin, S. L. (2003). Water content estimation in vegetation with MODIS reflectance data and model inversion models. *Remote Sensing of Environment*, 85, 109–124.